International Journal of Fluid Machinery and Systems
Vol. 2, No. 3, July-September 2009

Original Paper

Experimental Investigation on Separated Flows of Axial Flow Stator and Diagonal Flow Rotor

Yoichi Kinoue[1], Norimasa Shiomi[1], Toshiaki Setoguchi[2] and Yingzi Jin[3]

[1]Department of Mechanical Engineering, Saga University
1, Honjo, Saga, 840-8502, Japan
[2]Institute of Ocean Energy, Saga University
1, Honjo, Saga, 840-8502, Japan
[3]Institute of Mechatronics, Zhejiang Sci-Tech University
Xiasha Higher Educational Zone, Hangzhou, 310018, China

Abstract

Experimental investigations were conducted for the internal flows of the axial flow stator and diagonal flow rotor. Corner separation near the hub surface and the suction surface of stator blade are mainly focused on. For the design flow rate, the values of the axial velocity and the total pressure at stator outlet decrease between near the suction surface and near the hub surface by the influence of corner wall. For the flow rate of 80-90% of the design flow rate, the corner separation of the stator between the suction surface and the hub surface is observed, which becomes widely spread for 80% of the design flow rate. At rotor outlet for 81% of the design flow rate, the low axial velocity region grows between near the suction surface of rotor and the casing surface because of the tip leakage flow of the rotor.

Keywords: Axial flow stator, Diagonal flow rotor, Internal flow, Corner separation

1. Introduction

In the case of high loading or partial flow rate of an axial compressor stator flow, a separated region exists in the corner between the blade suction surface and the hub wall as shown in Fig. 1, which is so called a corner stall or a corner separation. That kind of flow is highly three-dimensional viscous flow, which has a profound influence on the performance of the blade rows.

Several studies concerning the three-dimensional separated flow in an axial compressor stator have been reported. Joslyn and Dring [1] investigated the flow in an stator with high loading and low aspect ratio. A stalled region with high aerodynamic loss in the corner of the suction surface and the hub wall was reported. Dong et al. [2] investigated flow and loss mechanism in a single-stage low-speed axial compressor stator. Large separated areas were observed at both near the hub and near the casing. Schlz and Gallus [3] performed detailed flow measurement in an isolated subsonic axial compressor stator at various blade loading. Blade and endwall visualization, blade boundary layer investigations with hot wires and hot films, and five-hole probe measurements were done at stator outlet. Corner separations both near the hub and near the casing were observed for some case. On the other hand, Hah and Loelbach [4] performed the steady RANS analysis and incorporated their numerical results and the experimental results of Schlz and Gallus [3] in order to advance the understanding of the basic mechanism of compressor hub corner stall. A twisterlike vortex was observed near the rear part of the stator blade suction surface.

The main purpose of this study is to investigate experimentally the separated flow of rear stator cascade in the diagonal flow fan, which can be considered as similar to an axial compressor stator. A corner separation near the hub surface and the suction surface of the stator blade is especially focused on. Also, the separated flow of the diagonal flow is experimentally investigated.

2. Experimental Apparatus and Procedure

Figure 2 shows the experimental apparatus in Saga University. By using this apparatus, the stage performance was evaluated as a combination of the rotor and the stator. The total pressure-rise of the stage was obtained from the pressure difference between the inlet chamber and the pressure tap which locates upstream of the damper. The torque was measured using a torque meter mounted

Received July 22 2009; accepted for publication August 5 2009: Review conducted by Prof. Yulin Wu. (Paper number O09025)
Corresponding author: Yoichi Kinoue, Associate Professor, kinoue@me.saga-u.ac.jp

Table 1 Specification of fan

Rotational speed		3100[min -1]
Design total pressure coefficient		0.345
Design flow rate coefficient		0.345
Type number		3.10
Duct diameter		380[mm]
Vortex pattern		Free vortex
Hub ratio		0.6
Inclination angle of hub		40[deg]
Inclination angle of casing		20[deg]
Rotor	Number of blade	6
	Max blade thickness chord length rate	Tip 5% Hub 10%
	Blade profile	NACA65
Stator	Number of blade	11
	Max blade thickness chord length rate	1%
	Blade profile	Circular arc blade

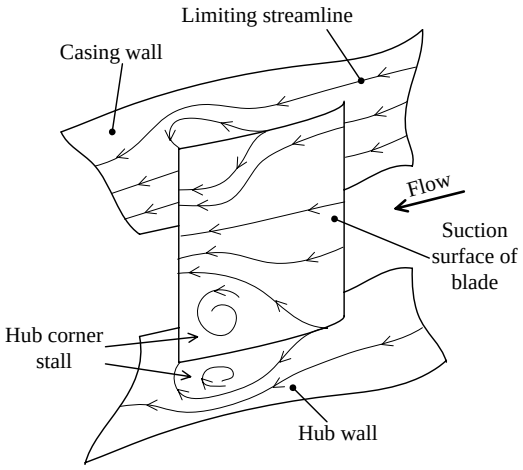

Fig. 1 Hub corner separation of stator

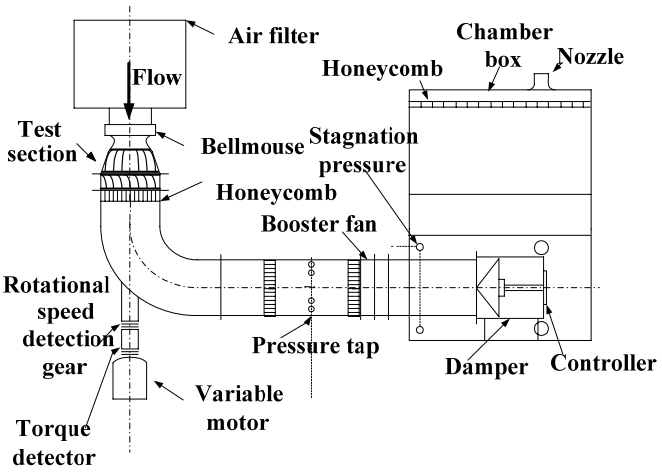

Fig. 2 Experimental apparatus

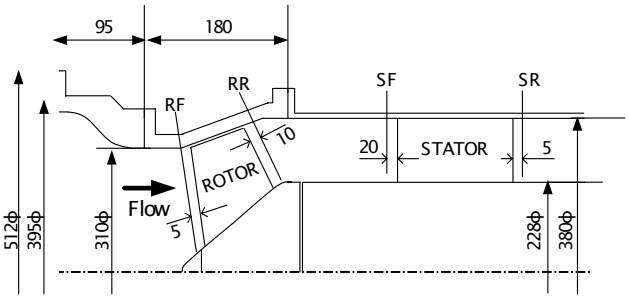

Fig. 3 Test section

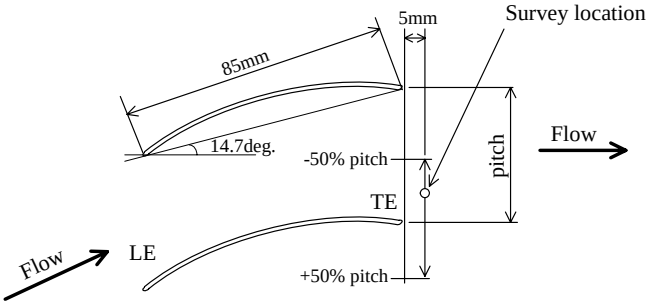

Fig. 4 Survey location at the back of stator

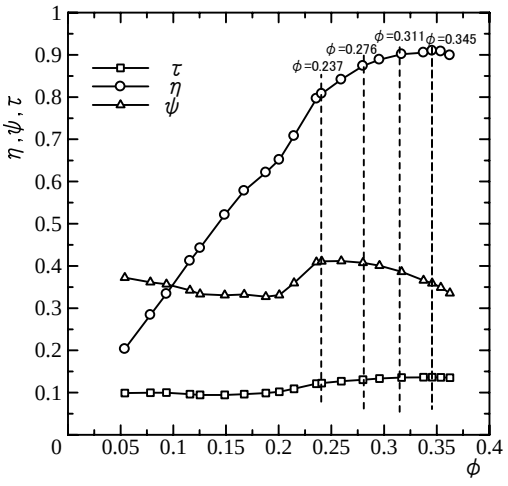

Fig. 5 Stage performance test

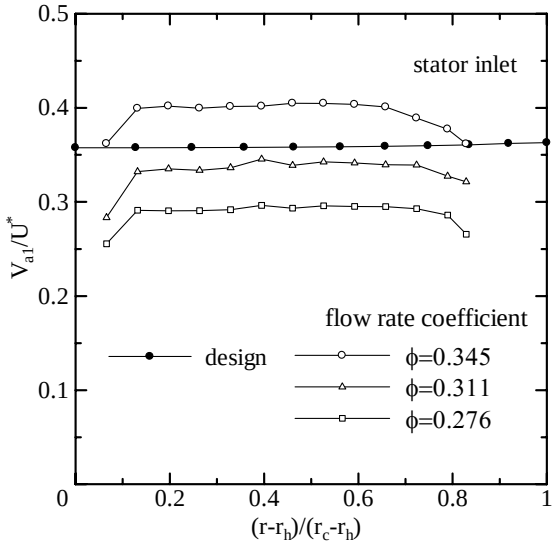

(a) stator inlet

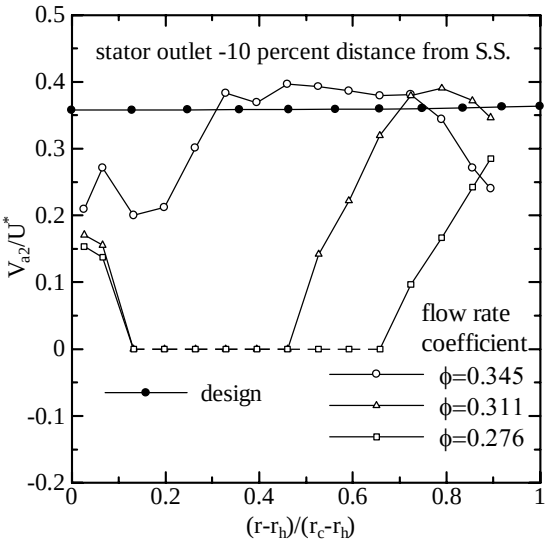

(c) stator outlet at -10% pitch

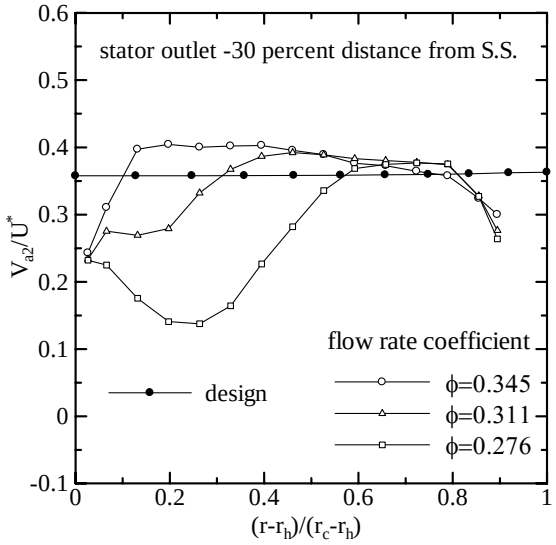

(b) stator outlet at -30% pitch

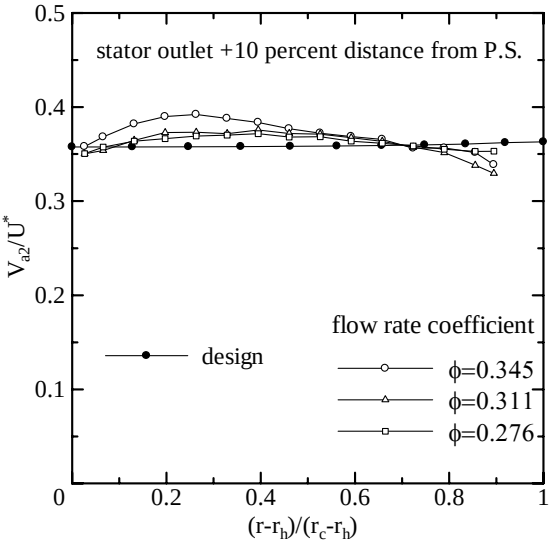

(d) stator outlet at +10% pitch

Fig. 6 Axial velocities at stator inlet and outlet

on rotor shaft. The test Reynolds number is about 4.39×10^5 based on the blade chord length at mid-span and blade tip speed at leading edge.

Table 1 shows the specification of fan tested. The rotor comprises 6 blades designed by the use of a quasi three-dimensional method based on two-dimensional NACA65 cascade data. The stator comprises 11 blades, of which the blade element selection was carried out by using two-dimensional cascade data of circular-arc blade. The tip clearance of rotor is 0.5 mm and the clearance of stator between the casing is 1.0 mm, which means that the stator is cantilevered by the hub wall.

Figure 3 shows the test section of the apparatus. The measurement of internal flow of the stator was conducted by using five-hole probe which is calibrated in advance. The axial location of measurement for stator were 20 mm upstream and 5 mm downstream of the leading edge and trailing edge, respectively. Fig. 4 shows the survey location at the back of stator. The circumferential survey locations at stator outlet were set from -50 % to +50 % pitch, where the minus sign means suction surface side and the plus sign means pressure surface side, respectively. Uncertainties of velocity magnitude and angle of this five-hole probe was estimated as 0.45 m/s and 3.1 degrees.

The measurement of internal flow of the rotor was conducted by using hot wire probe calibrated in advance. At the outlet of the rotor, phase-locked values were measured by using phase-locked averaging technique [5]. Uncertainties of velocity magnitude and angle of this hot wire probe was estimated as 0.52 m/s and 3.2 degrees.

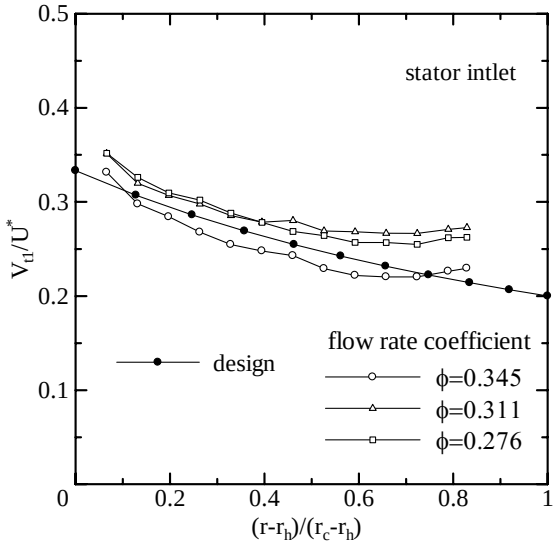

(a) stator inlet

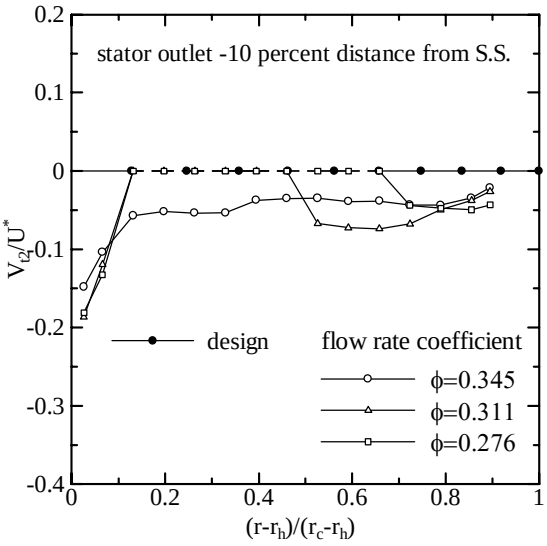

(c) stator outlet at -10% pitch

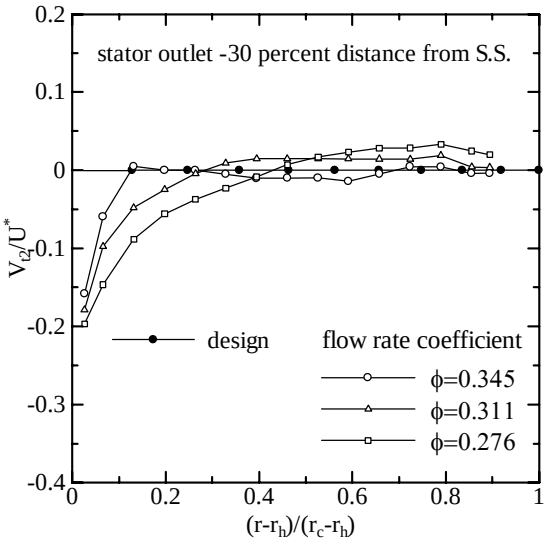

(b) stator outlet at -30% pitch

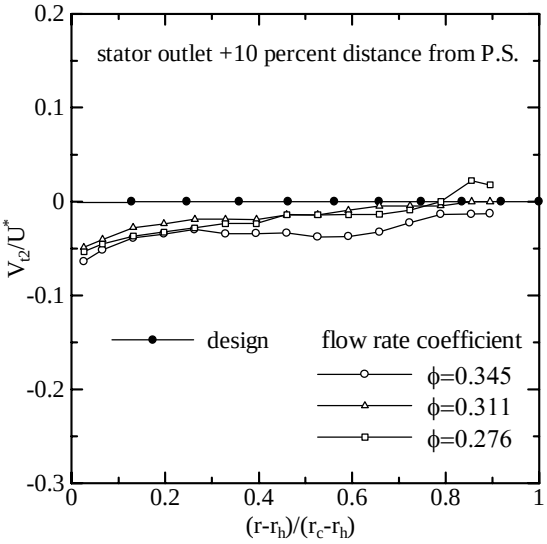

(d) stator outlet at +10% pitch

Fig. 7 Tangential velocities at stator inlet and outlet

3. Experimental Results and Discussions

3.1 Stage Performance Test

Figure 5 shows the characteristic curves of the test fan. Total pressure efficiency η, total pressure-rise coefficient ψ and torque coefficient τ are plotted against flow-rate coefficient ϕ. These values are defined as follows.

$$\phi = Q/\left(AU^*\right) \tag{1}$$

$$\psi = \Delta P/\left(\rho U^{*2}/2\right) \tag{2}$$

$$\tau = T\omega/\left(\rho U^{*3}A/2\right) \tag{3}$$

$$\eta = \phi\psi/\tau \tag{4}$$

Where, $A=\pi\,(D_c^2-D_h^2)/4$ and U^* is the reference velocity, that is, $U^*=D_c\omega/2$.

Experimental value of ψ at design flow rate coefficient ϕ=0.345 agrees well with the design value ψ=0.345. Experimental value of η at ϕ=0.345 takes η =90.3 %. The value of ψ takes maximum at around ϕ=0.25. The internal flow measurement of stator were done by using five-hole probe for ϕ=0.345 (ϕ_{design}), ϕ=0.311 (0.9 ϕ_{design}) and ϕ =0.276 (0.8 ϕ_{design}), respectively. Further, the measurement of rotor flow were done by using hot wire probe for ϕ_{design}, 0.92 ϕ_{design} and 0.81 ϕ_{design} , respectively.

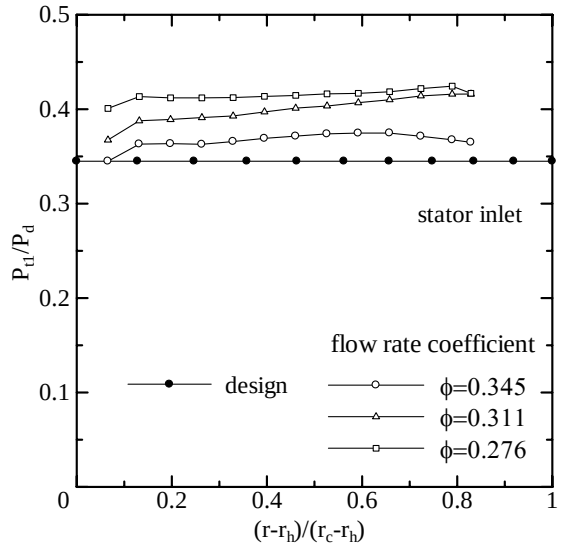

(a) stator inlet

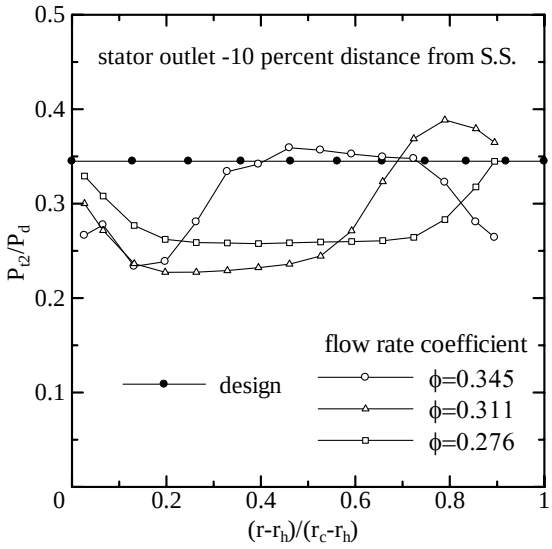

(c) stator outlet at -10% pitch

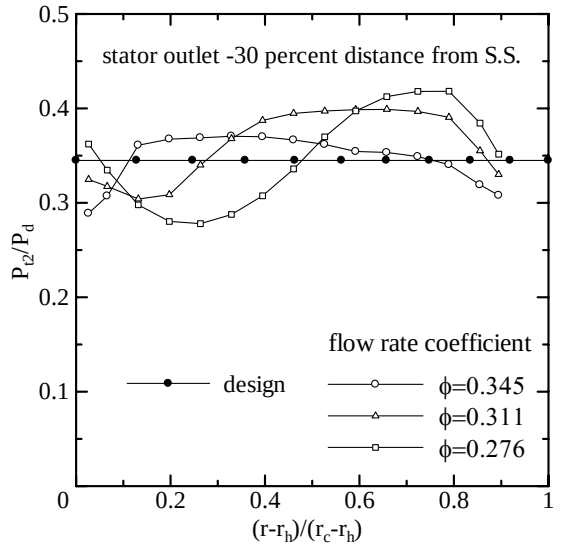

(b) stator outlet at -30% pitch

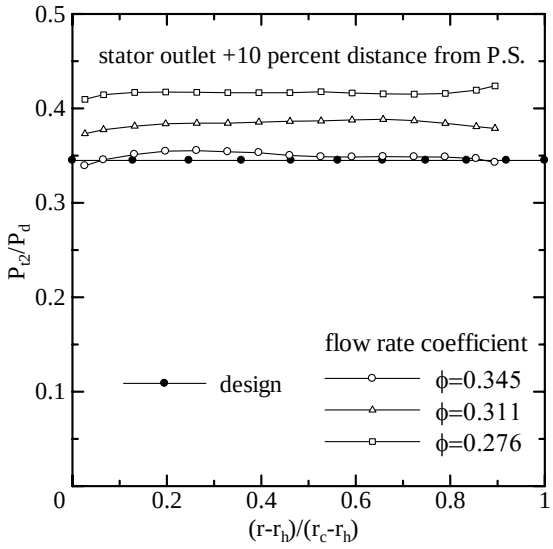

(d) stator outlet at +10% pitch

Fig. 8 Total pressures at stator inlet and outlet

3.2 Stator Flow for Design Flow Rate

Figures 6, 7 and 8 show the measurement results by using five-hole probe both at stator inlet and outlet for ϕ=0.345 (ϕ_{design}), ϕ=0.311 (0.9 ϕ_{design}) and ϕ =0.276 (0.8 ϕ_{design}), respectively. In Fig. 6, axial velocity V_a is normalized by the reference velocity U^*. Tangential velocity V_t in Fig. 7 is also normalized by U^* and negative value of V_t means overturning of the flow. In Fig. 8, total pressure P_t is normalized by the dynamic pressure P_d in which the reference velocity is used. In all the figures of Figs. 6-8, the radius r is normalized by the values of the hub r_h and casing r_c. The ratio of circumferential distance from the trailing edge location of the stator varies from -50% (suction side) to +50% (pressure side).

In Fig.6 for ϕ=0.345, in the case of -30% of the circumferential location (Fig. 6(b)), the profiles of V_a / U^* is almost uniform except near the walls. The values P_t / P_d for the same condition (ϕ=0.345 and -30% pitch) in Fig. 8(b) has also uniform profile and is close to the value of 0.345 of the design value. The value of V_t / U^* for ϕ=0.345 and -30% pitch in Fig. 7(b) is close to the value of 0 of the dssign value except near the hub region, where the flow is overturning because of the secondary flow.

When the circumferential location approaches to the suction surface (-10% pitch), the values of V_a / U^* in Fig. 6(c) and P_t / P_d in Fig. 8(c) decrease at around the hub surface by the influence of the corner walls. The value of V_t / U^* in Fig. 7(c) is negative for full span and is large negative value near the hub.

3.3 Stator Flow for Partial Flow Rate

In the case of 90% of the design flow rate (ϕ=0.311), in Fig. 6(c) of -10% pitch case, axial velocity V_a can not be measured because of little difference of five pressures, therefore the value of 0 are plotted and the line becomes broken in such the cases.

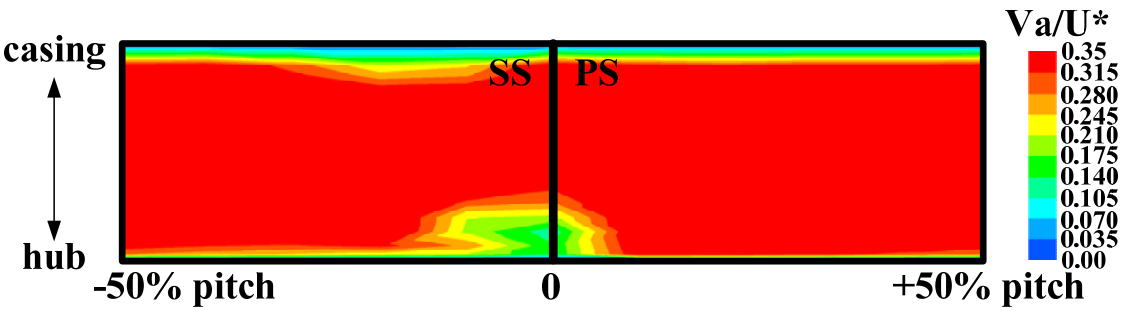

(a) ϕ=0.345 (ϕ_{design})

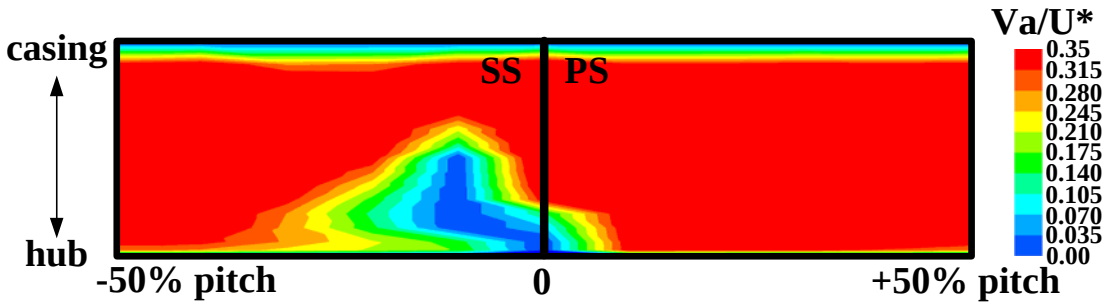

(b) ϕ=0.311 (0.9ϕ_{design})

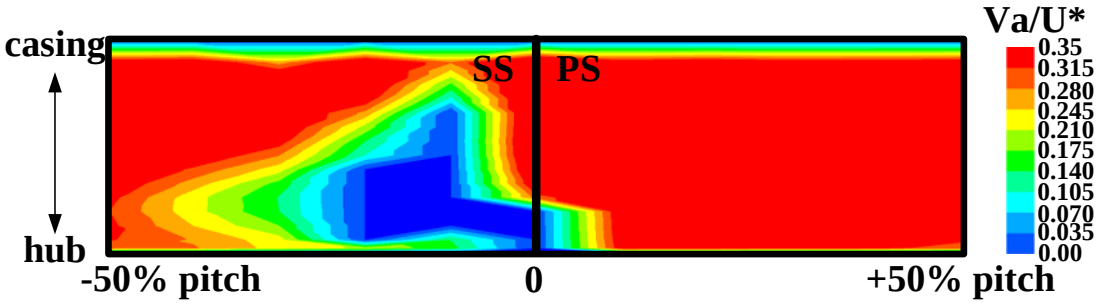

(a) ϕ=0.276 (0.8ϕ_{design})

Fig. 9 Contour maps of normalized axial velocity at stator outlet (five-hole survey)

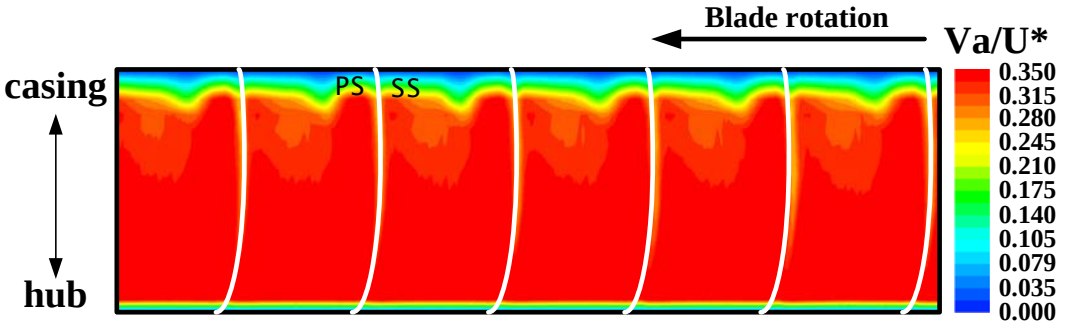

(a) ϕ=0.345 (ϕ_{design})

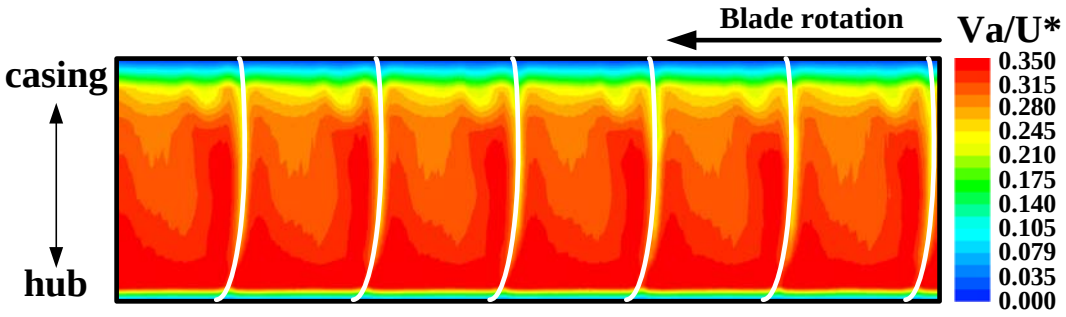

(b) ϕ=0.317 (0.92ϕ_{design})

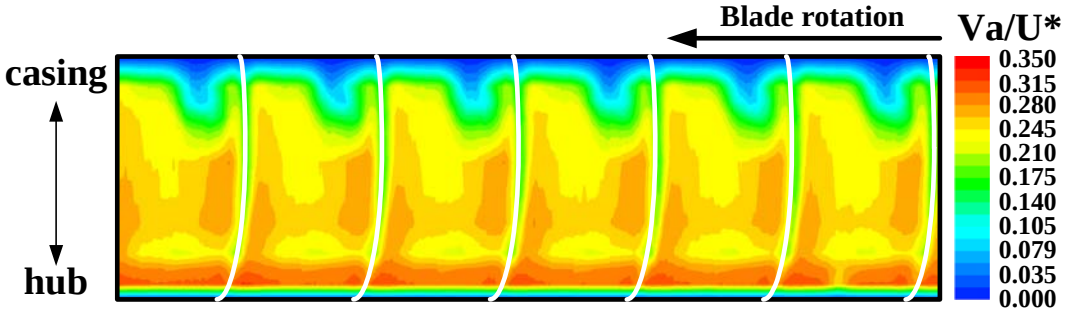

(c) ϕ=0.280 (0.81ϕ_{design})

Fig. 10 Contour maps of normalized axial velocity at rotor outlet (hot-wire survey)

The flow seems separated from hub to mid region at -10% pitch location for ϕ=0.311. In Fig. 6(b) of -30% pitch case for ϕ=0.311, the region of small V_a/U^* values can be also seen near the hub. The values of P_t / P_d in Fig. 8(b) and (c) also show similar tendency of corner separation.

In the case of 80% of the design flow rate (ϕ =0.276), the separation region becomes widely spread to near the casing.

3.4 Contour Map at Stator Outlet

Figure 9 shows contour maps of V_a / U^* at stator outlet, which is measured by using five-hole probe. Radial and circumferential geometries are transformed to rectangle geometries. This measured surface is observed from upstream and the thick black line, PS and SS show the trailing edge of stator, the pressure surface and the suction surface, respectively. The colors of blue and red means the value of 0.0 and 0.35 but the blue area in the top part of each figure is due to the lack of information.

In Fig. 9(a) for ϕ=0.345 (ϕ_{design}), a small corner separation can be found at the corner between the hub surface and the suction surface of the blade. Also, the region of small V_a / U^* value can be seen near the casing of suction side, which can be considered as the influence of tip leakage flow of stator.

In Fig. 9(b) for ϕ=0.311 (0.9ϕ_{design}), the region of small V_a / U^* value grows up to mid-span and further in Fig. 9(c) for ϕ=0.276 (0.8ϕ_{design}), small value of V_a / U^* approaches near the casing and near the mid-pitch location (-50% pitch).

3.5 Contour Map at Rotor Outlet

Figure 10 shows contour maps of V_a / U^* at rotor outlet, which is measured by using hot wire probe. Similar to the stator case, geometries are transformed to rectangle and the measured surface is observed from upstream. The direction of blade rotation, the pressure and suction surface are shown in the figure. The data of hot wire are averaged by phase-locked to the rotor blade [5]. The colors of blue and red means the value of 0.0 and 0.35 but the blue area in the top part of each figure is due to the lack of information.

In Fig. 10(a) for ϕ_{design} and 10(b) for 0.92ϕ_{design}, only a small region of low velocity can be observed, which can be considered as the influence of tip leakage flow of the rotor. In Fig. 10(c) for 0.81ϕ_{design}, the low velocity region grows at around between the suction surface and the casing surface.

4. Conclusion

Experimental investigation on the separated flows of axial flow stator and diagonal flow rotor were conducted. Corner separation near the hub surface and the suction surface of the stator blade are mainly focused on. Conclusions are summarized as follows.

(1) Experimental value of total pressure-rise coefficient in the performance test for design flow rate agrees well with the design values, and the efficiency for design flow rate is 90.3%.

(2) At stator outlet for design flow rate, the values of axial velocity and the total pressure decrease between near the suction surface of the blade and the hub surface by the influence of the corner wall.

(3) At stator outlet for 80-90%of the design flow rate, the corner separation between the suction surface and the hub surface can be found which becomes widely spread for 80% of the design flow rate.

(4) At rotor outlet for 81% of the design flow rate, the low axial velocity region grows between near the suction surface and the casing surface because of the tip leakage flow of the rotor.

Acknowledgments

The authors wish to acknowledge the cooperation to Dr. K. Kaneko, Honorary Professor of Saga University. Also, authors sincerely acknowledge the financial support 2006 for this research by Harada Memorial Foundation.

Nomenclature

A	Reference area [m^2]	ϕ	Flow rate coefficient [-]
D_c	Casing diameter [m]	η	Total pressure efficiency [-]
D_h	Hub diameter [m]	ρ	Density of air [kg/m^3]
ΔP	Total pressure-rise [Pa]	τ	Torque coefficient [-]
P_t	Total pressure [Pa]	ω	Angular velocity [1/s]
Q	Volumetric flow rate [m^3/s]	ψ	Total pressure-rise coefficient [-]
r	Radius [m]		
T	Torque [Nm]		
U^*	Reference velocity [m/s]		
V_a	Axial velocity [m/s]		
V_t	Tangential velocity [m/s]		

References

[1] Joslyn H.D. and Dring R., 1985, “Axial Compressor Stator Aerodynamics,” ASME Journal of Engineering for Gas Turbines and Power Trans. ASME, Vol. 107, pp. 485-493.

[2] Dong Y., Gallimore S.J. and Hodoson H.P., 1987, “Three-Dimensional Flows and Loss Reduction in Axial Compressors, “ Journal of Turbomachinery Trans. ASME, Vol. 109, pp. 354-361.

[3] Schlz H.D. and Gallus H.D., 1988, “Experimental Investigation of the Three-Dimensional Flow in Annular Compressor Cascade,” Journal of Turbomachinery Trans. ASME, Vol. 110, pp. 467-478.
[4] Hah C. and Loellbach J., 1999, “Development of Hub Corner Stall and Its Influence on the Performance of Axial Compressor Blade Rows”, Journal of Turbomachinery Trans. ASME, Vol. 121, pp. 67-77.
[5] Kuroumaru, M., Inoue, M., Higaki, T., Abd-elaziz, F. A. and Ikui, T., 1982, “Measurement of Three-Dimensional Flow Field behind an Impeller by Means of Periodic Multi-Sampling of a Slanted Hot Wire,” Bulletin of the JSME, Vol. 25, No. 209, pp. 1674-1681.